Intrinsic Dynamics and Condition Dependence of Homogeneous Ester Hydrogenation Revealed by Mn-CNC Pincers

Wenjun Yang,[a] Tejas Y. Kalavalapalli,[a] Annika M. Krieger,[a] Taras A. Khvorost,[b] Ivan Yu. Chernyshov,[b] Manuela Weber,[c] Evgeny A. Uslamin,[a] Evgeny A. Pidko,*[, a,b] Georgy A. Filonenko*[, a]

[a] Inorganic Systems Engineering group, Department of Chemical Engineering, Faculty of Applied Sciences, Delft University of Technology, Van der Maasweg 9, 2629 HZ, Delft, The Netherlands

[b] TheoMAT Group, ChemBio cluster, ITMO University, Lomonosova 9, St. Petersburg, 191002, Russia

[c] Institute of Chemistry and Biochemistry, Freie Universität Berlin, Fabeckstraße 34/36, Berlin, D-14195, Germany

Corresponding authors: Georgy A. Filonenko (G.A.Filonenko@tudelft.nl)

Evgeny A. Pidko (E.A.Pidko@tudelft.nl)

Abstract: Homogeneous catalytic hydrogenations often operate in dynamic conditions. For example, in hydrogenation of esters reaction medium changes its polarity and becomes protic as reaction proceeds. As a result, the nature of the catalytic and reactive species in catalysis can change throughout the reaction, making it impossible to draw a static picture describing the catalyst performance. Herein we report on the molecular origins of such a complexity in the catalytic hydrogenation of esters. Using a new bis-N-heterocyclic carbene manganese (I) pincer catalyst we perform operando FTIR spectroscopy and kinetic studies to reveal the highly dynamic nature of the Mn intermediates formed in the catalytic mixture. Furthermore, we identify persistent inhibition phenomena caused by the reversible interaction of catalytically competent species with alcohol products. Pronounced strongly in Mn-promoted hydrogenation, this inhibitory pathway can principally affect any transition metal catalyst in ester hydrogenation. Finally, we show that the catalyst inhibition can be suppressed by using basic alkoxide promotors common for the majority of polar hydrogenations. We provide the first experimental and computational evidence that alkoxide promotion can alter the shape of the free energy surface and render catalyst inhibition unfavorable. At large, it implies a marked change to the values of the standard free energies of the key steps in the catalytic cycle that are universally assumed to be constant. While allowing to promote transformations that would otherwise be thermodynamically prohibited, these phenomena make a case for reconsideration of a traditional static viewpoint on homogeneous hydrogenation reactions.

Introduction

Catalytic hydrogenations comprise a vast class of reactions with high industrial relevance.[1] Utilizing molecular hydrogen with appropriate catalyst, these reactions can convert unsaturated functional groups in a variety of substrates to their saturated counterparts. Out of numerous functional groups that can be reduced in this way, our work examines hydrogenation of esters, polar substrates posing significant challenge for direct catalytic hydrogenation.[2]Conversion of esters to alcohols via catalytic hydrogenation have been explored for several decades with the most prominent homogeneous catalysts for this transformation being bifunctional noble metal complexes of ruthenium[3], iridium[4], and osmium[5]. Recent years have seen the focus of catalytic community shifting towards utilizing early transition metal (TM) catalysts, viewed as sustainable and non-toxic alternatives for noble metals.[6] First found for iron and cobalt, ester hydrogenation activity was recently discovered for manganese complexes that are the focus of our work. While the manganese catalysts offer high sustainability benefits, their performance rarely matches that of noble metals.[7] The best examples of Mn catalysts for hydrogenation of esters still require high catalyst loadings >2000 ppm and often operate at temperatures and pressures up to 110 C and 50 bar to achieve high conversion.[8] The search

for the new, more reactive Mn complexes with high intrinsic reactivity remain the focal point in this field.

However, the reactivity alone is not sufficient to forecast catalytic performance since catalysis is a complex and dynamic phenomenon. A growing evidence suggests that the reactivity of catalytic species can significantly vary depending on reaction conditions. Our group, for example, demonstrated that reaction medium composition can directly impact reactivity patterns in homogeneous catalysis.[9] Similarly, in heterogeneous catalysis, Liu, Lercher and co-workers demonstrated that local solvation and ionic strength changes can alter the reactivity of zeolite catalysts.[10] In the case of ester hydrogenation, reaction conditions change dramatically with reaction medium changing from aprotic to highly protic. Whether this change can steer the catalyst reactivity remained unknown and resolving this question and its molecular origins was the aim of this work.

Using a combination of operando spectroscopy[11], DFT calculations and stoichiometric reactivity studies we demonstrate that composition and relative content of catalytic species during hydrogenation is not constant but dynamic. This dynamics is largely caused by the change in reaction mixture composition during ester hydrogenation wherein the growing fraction of reaction product causes catalyst inhibition. We directly demonstrate that kinetically competent catalysts species are in equilibrium with inhibited catalyst formed through a reaction with hydrogenation product. Strikingly, we found reaction conditions can directly affect this equilibrium. Specifically, addition of basic promotors could change the *standard* thermodynamic parameters of inhibitory equilibrium and make this inhibition unfavorable. Considering that standard thermodynamic potentials are universally assumed constant, our discovery of their condition dependence makes a strong case that catalytic reactions are inherently dynamic on every level: from molecules to environment fundamentals.

Results and Discussion

Catalyst design

To demonstrate the impact of changing reaction conditions we developed new Mn pincer catalysts for ester hydrogenation that were both catalytically competent and easy to track using spectroscopic methods. We based our model catalysts design on bis-N-heterocyclic carbene amino (CNC) pincer ligands that proved to be a versatile motif for transition-metal hydrogenation catalysts.[3d, 12] The representative ligand **1** readily undergoes complexation with $Mn(CO)_5Br$ in the presence of the phosphazene base BEMP in acetonitrile at 80 °C yielding Mn complexes **2** and **3** (Figure 1) as a mixture of isomers. As evidenced by X-ray diffraction data, the CNC ligand in these complexes adopts *facial* and *meridional* configurations for **2** and **3** respectively (Figure 2). Exposure to ambient light slowly converts complex **2** to **3** in solution implying that **2** might be a kinetic product of the complexation.[8a] Both

complexes are cationic tricarbonyl species that are readily distinguished by ^{1}H NMR and IR spectroscopy (see section S2 of Supporting Information).

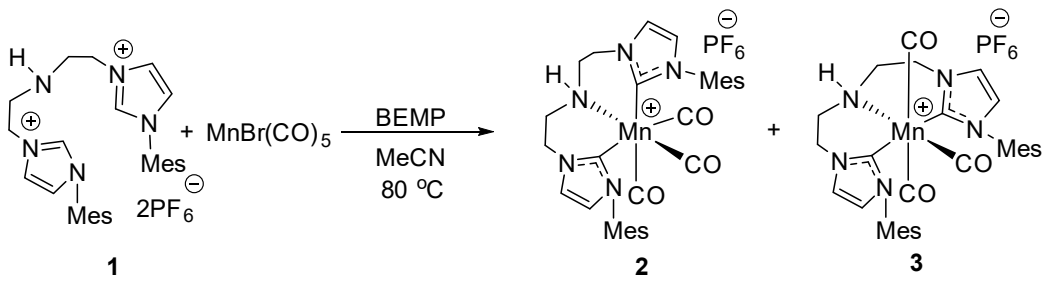

Figure 1. Synthesis of Mn(I) complexes **2** and **3**.

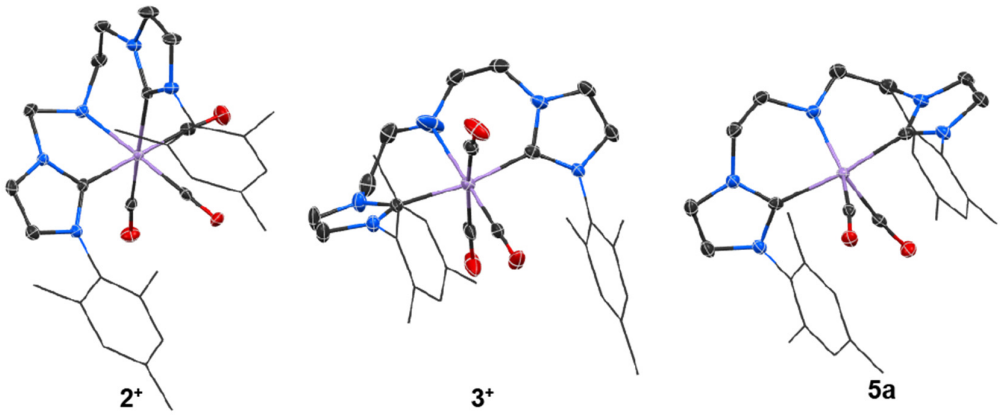

Figure 2. Molecular structure of complexes **2**, **3**, and **5a** in the crystal with thermal ellipsoids drawn at 50% probability. Hydrogen atoms and PF_6 anions in cationic **2** and **3** are omitted for clarity.

Similar to other amine centered pincers, **2** and **3** exhibit reactivity towards strong bases.[6a, 6b, 6d, 6g, 6h, 13] Namely, reaction with KO^{t}Bu in THF (Figure 3) rapidly converts *meridional* **3** to a corresponding dicarbonyl complex that apparently exists as a mixture of two species evidenced by IR spectroscopy indicating the presence of new CO bands at 1886, 1811 and 1858, 1771 cm^{-1}, corresponding to dicarbonyl Mn amido species **5a** and its KO^{t}Bu adduct **5b**, respectively. A deep blue coloration of **5a** implies a significant change of the electronic structure of this complex that we assigned to a change of octahedral to trigonal bipyramidal geometry found in some neutral Mn amidocomplexes.[14] Using IR spectroscopy we found that deprotonation of *fac* complex **2** also leads to **5a/b** mixtures but proceeds in a stepwise manner with the transient formation of yellow neutral tricarbonyl complex **4** that loses CO within hours. Although further treatment of **5a/b** mixtures with H_2 did not yield detectible amounts of Mn hydride species, we observed the rapid conversion of **5a/b** mixture to pure **5a** under 5 bar of H_2 suggesting that complex **5b** is a metastable species and sensitive to weak proton donors (see Figure S23). Complex **5a**, being the end point of this reactivity pathway regardless of Mn complexes used,

could be isolated and characterized with X-ray diffraction that confirmed the bipyramidal geometry of **5a** with N-Mn-CO angles of 141° and 135° typical for dicarbonyl complexes of this geometry (Figure 2). A comprehensive conformational analysis of the deprotonated $Mn(CO)_2CNC$ complexes and its adduct with a model alkoxide base was carried out by DFT calculations (see section S10 of Supporting Information) to confirm our spectral assignments. Computations reveal that interaction with potassium alkoxide can indeed stabilize some of the metastable conformers of $Mn(CO)_2CNC$ produced upon the deprotonation of the fac-complex **4** to form adducts with computed ν(CO) similar to those experimentally observed for the metastable potassium adduct **5b**, therefore supporting its proposed structure.

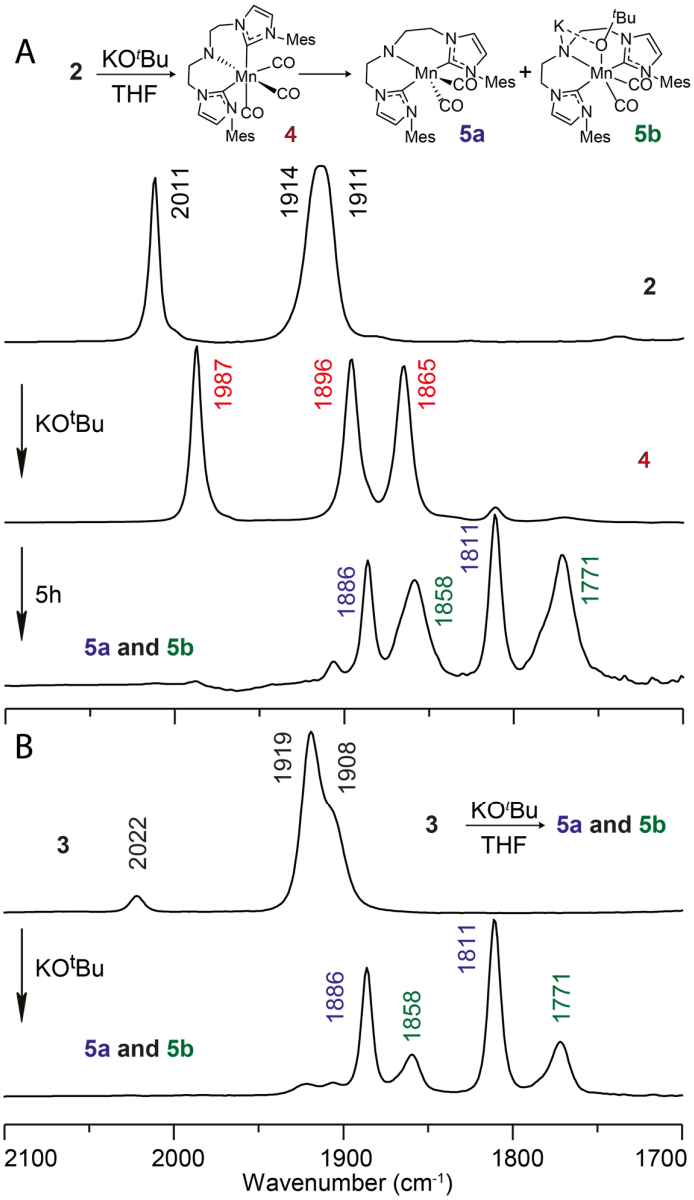

Figure 3. FTIR spectroscopy data for reactions of precatalysts **2** and **3** with alkoxide bases.

The new MnCNC complexes **2** and **3** are active in ester hydrogenation. As expected, reduction of ethyl hexanoate benchmark substrate with **2** and **3** gave nearly identical conversion confirming the catalytic equivalency of these precatalysts (see Table S1) and prompting us to use complex **2** in all further studies. The most peculiar feature of ester hydrogenation with **2** is its reliance on the base promotor for remaining active. While the trace amounts of alcohol product were obtained with 1 mol% KO^{t}Bu, increasing its amount to 10 and 20 mol% significantly increased hexanol yield to 41% and 46% respectively (Table 1, entries 1–3). An increase in catalyst loading and temperature (Table 1, entries 4–6) proved beneficial for catalytic performance with 87% yield reached at 90 °C with 0.2 mol% complex **2**. Importantly, further increase of reaction temperature to 100 °C proved detrimental and yielded mere 8% of hexanol product. At this temperature, decreasing the amount of base to 10 mol% restored the catalytic efficiency (88% yield, entry 7) and rendered the catalytic system sufficiently stable to reach nearly quantitative hexanol yield in prolonged run (entry 8).

Table 1. Hydrogenation of ethyl hexanoate with **2** under varied reaction conditions.[a]

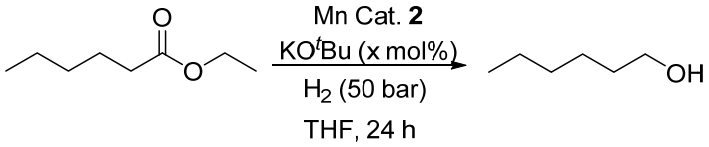

Entry	T (°C)	**2** (mol%)	x (mol%)	Conv. (%)	Yield (%)
1	80	0.1	1	< 1	<1
2	80	0.1	10	63	41
3	80	0.1	20	67	46
4	80	0.2	20	77	65
5	90	0.2	20	92	87
6	100	0.2	20	22	8
7	100	0.2	10	93	88
8[b]	100	0.2	10	99	98

[a] Conditions: ethyl hexanoate (1.25 mmol), Mn catalyst **2**, KOtBu, THF (0.5 mL), P = 50 bar H_2, t = 24 h. Conversion and yield determined by GC analysis with dodecane as internal standard. [b] Reaction was run for 48 h

Our screening data highlight the importance of base promoter for catalytic activity of **2** and point that superstoichiometric amount of base with respect to the Mn catalyst may be necessary to complete the hydrogenation reaction. This behaviour is not uncommon and a number of Mn hydrogenation catalyst systems is known to utilize superstoichiometric amounts of alkoxide bases far beyond those necessary for precatalysts activation per se.[7i, 7m, 7n, 7w, 8a, 8c-e, 15] This requirement is not limited to Mn complexes as

many noble metal hydrogenation catalysts are also incapable of a purely base free operation. [3a-f, 4a, 5, 16]

Mechanistic analysis

The unusual sensitivity of the catalytic hydrogenation to the base promoter prompted us to perform a series of operando studies monitoring hydrogenation kinetics simultaneously tracking the composition of the reaction mixture with IR spectroscopy. A typical dataset produced in this study is depicted in Figure 4. Examining the evolution of the carbonyl ligands in **2** in the course of reaction we note that the reaction onset is marked by the fast consumption of the base-adduct **5b** and the formation of the amido complex **5a** as the major species in the reaction mixture (Figure 4A). As the hydrogenation progressed and the alcohol product formed we observed a gradual consumption of **5a** and the formation of a new species **6** with ν(CO) = 1902, and 1806 cm^{-1} suggesting that **6** is a Mn dicarbonyl complex. Performing an ex-situ test to assign the structure of **6** we found that this complex is the product of the metal-ligand cooperative alcohol addition to the amido complex **5a** (Figure 4C). Using methanol as a model alcohol we could obtain reference FTIR and NMR spectra for the alkoxide **6** and establish the reversibility of its formation with the alkoxide being favored at low temperature and the amido complex **5a** favored at elevated temperatures (see Figures S24–27).

Examining the real-time FTIR data we noted that the kinetics of the **5a** consumption cohered well with the changes in the overall catalytic hydrogenation rate during the reaction (Figure 4B). If the two are indeed correlated, we assumed that the alcohol product formation is responsible for the consumption of the amido complex **5a** thereby diminishing the steady state concentration of the kinetically competent species. This behavior implies a profound product-induced inhibition throughout the catalytic reaction. As the IR spectroscopy cannot distinguish between the ethanol and hexanol adducts of **5a** we studied the hydrogenation of hexyl hexanoate – a substrate producing two identical alcohol molecules upon the hydrogenation, so that all Mn-alkoxide species would be identical. We additionally incorporated a two-hour activation step of the Mn precatalyst under H_2 atmosphere at room temperature to ensure a complete conversion of the **5a/b** mixture to **5a** at the onset of reaction to fully eliminate the induction period (see Figures S31, 33, 35 and 37).

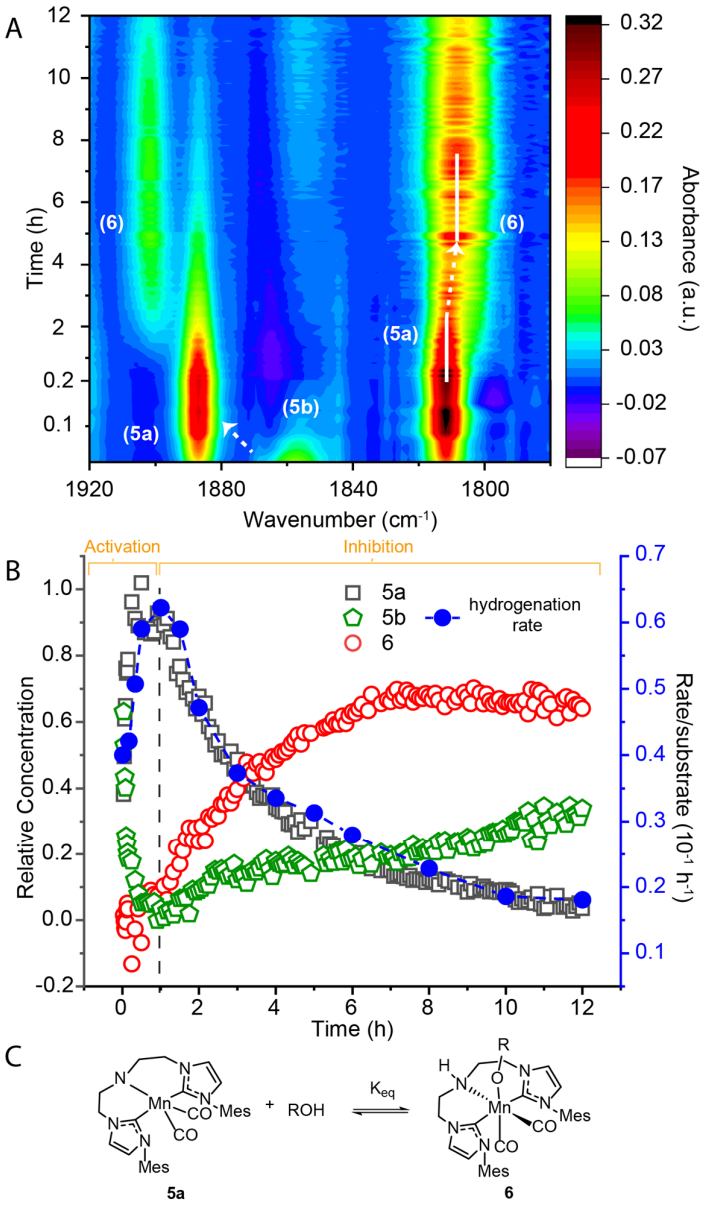

Figure 4. Operando FTIR results for the hydrogenation of ethyl hexanoate with Mn precatalyst **2**: A) Real-time FTIR spectrum in the carbonyl ligand stretching region (1920–1780 cm^{-1}); B) kinetic FTIR profile of complex **5a**, **5b**, and **6** plotted along with the catalytic rate profile; C) the metal-ligand cooperative activation of an ROH alcohol by the amido complex **5a** to form the Mn-alkoxide **6.**

Assuming the presence of the product inhibition we probed this phenomenon by performing hydrogenation in the presence of the hexanol product ($[HexOH]_0$ = 1.25 M at t = 0). Addition of alcohol strongly impacted the catalytic performance and the reaction mixture composition (Figure 5A). Firstly, we observed Mn alkoxide **6** to become the dominant Mn species from the onset of the reaction (Figure 5E *vs.* 5D). Secondly, we detected a significant drop in the hydrogenation rate compared to the

standard hexanol-free runs at the same substrate concentration (Figure 5B). These experiments confirm the detrimental impact of the product formation on catalysis and constitute a typical case of product inhibition. Interestingly, bulky and less acidic *tert*-butanol (see Figure 5A and Figures S34-35) did not inhibit catalysis notably in line with the absence of reactivity of this alcohol with **5a** that we observed ex-situ.

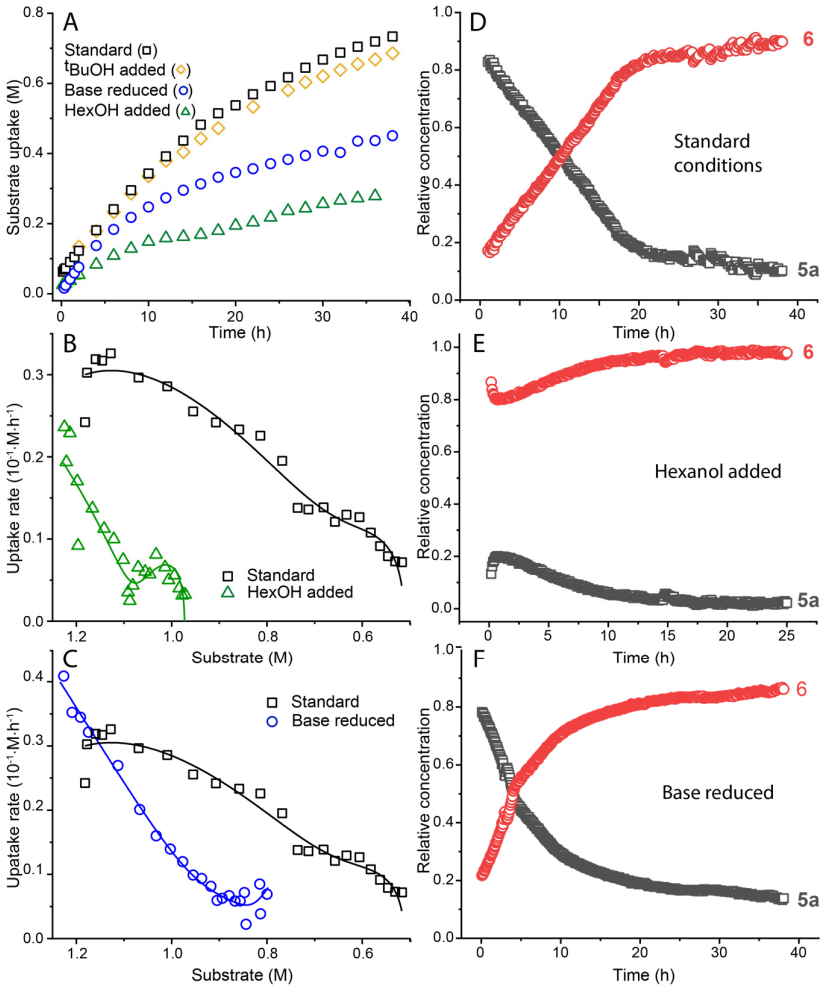

Figure 5. Operando FTIR spectroscopy studies on the product inhibition. Conditions - *standard*: hexyl hexanoate (1.25 M), Mn catalyst **2** (0.1 mol%), KO^{t}Bu (10 mol%) in THF (8.2 mL) at 70°C under 40 bar H_2; *hexanol/ ^{t}BuOH added*: extra alcohol added to 1.25 M; *reduced base:* KO^{t}Bu loading lowered to 2 mol%. A) substrate uptake *vs*. time; B, C) comparison of uptake rates at different reaction conditions; D, E, F) concentration of Mn species *vs.* time under different reaction conditions. *Notes:* uptake data in A-C determined by GC analysis, relative concentrations in D-F obtained from FTIR spectroscopy.

Assuming that the formation of alkoxide complexes is detrimental for catalysis we expected the magnitude of this effect to depend on the alcohol in question. Monitoring the equilibrium between **5a** and **6** with UV-Vis spectroscopy we could track the temperature dependence of the equilibrium constant and by extension the ΔG°_{298K} of this transformation. The blue complex **5a** has a characteristic

absorbance feature at 583 nm while its alcohol adduct **6** has a distinct feature at 428 nm (see section S9 of Supporting Information). We determined thermodynamic parameters of the alcohol adduct formation for three representative alcohols, namely, n-hexanol, methanol and benzyl alcohol (Table 2). We confirmed that more acidic alcohols, Me- and BnOH bind more favorably than hexanol with the measuredΔG°_{298K} being -13.5 and -11.3 kJ/mol for MeOH and BnOH, respectively, compared to -4.4 kJ/mol for hexanol. These data mimic the trends that we observed in our substrate scope screening (see Table S2) where methyl and benzyl esters consistently provided lower hydrogenation yields compared to their long chain counterparts (substrates **A7**, **A8**, and **A9**). Similarly, hydrogenation of aromatic esters (**A7**-**A10**) that produce benzyl alcohol as one of the products resulted in lower yields compared to the aliphatic esters (**A1**-**A6**) despite the latter being less electrophilic and less susceptible to the hydride transfer reactions often invoked as the first step in ester hydrogenation.

While it is unusual to observe the product induced inhibition of this magnitude, we find a broad agreement between our data and the literature examples for a wide range of hydrogenation catalysts. For example non-pincer MnPN complex reported by our group convert *tert*-butyl and ethyl esters with significantly higher efficiency compared to methyl counterparts.[8c] Similarly, RuCNC pincers reported by our group, RuPNP developed by the Gusev's group, and Ru-CNH_2 precatalysts synthesized by Morris and coworkers feature reduced efficiency towards aromatic esters.[3c, 3d, 5a, 17] At the same time, Zhang's group reported a hydrazine group-containing Ru pincer complex which gave profoundly diminishing yields of ester reduction as the medium changed from ^{i}PrOH to EtOH and MeOH.[18] Taken together, our observations suggest that the product induced inhibition observed above might direct the performance of a large number of hydrogenation catalysts or at least impact their productivity.

Table 2. Experimental and calculated thermodynamic parameters for the addition of alcohols to Mn amido complex 5a.

Alcohol	ΔG°_{298K} (kJ·mol^{-1})		$\Delta H°$ (kJ·mol^{-1})		$\Delta S°$ (J·mol^{-1}·K^{-1})	
	Experiment	Theory	Experiment	Theory	Experiment	Theory
MeOH	-13.5±0.8[a]	-0.2	-49.8±0.6	-32.9	-121.6±1.9	-113
HexOH	-4.4±1.0[a]	4.0	-36.2±0.7	-29.1	-106.9±2.5	-115
BnOH	-11.3±0.6[a]	-12.0	-40.5±0.4	-45.4	-97.9±1.3	-115

[a] Error from propagation of the error of $\Delta H°$ and $\Delta S°$, $\sigma_{\Delta G} = \sqrt{(\sigma_{\Delta H})^2 + (|T|\sigma_{\Delta S})^2}$. Errors in the enthalpy and entropy are from errors in the slope and intercept, respectively. Note: see discussion below for the details of theoretical analysis.

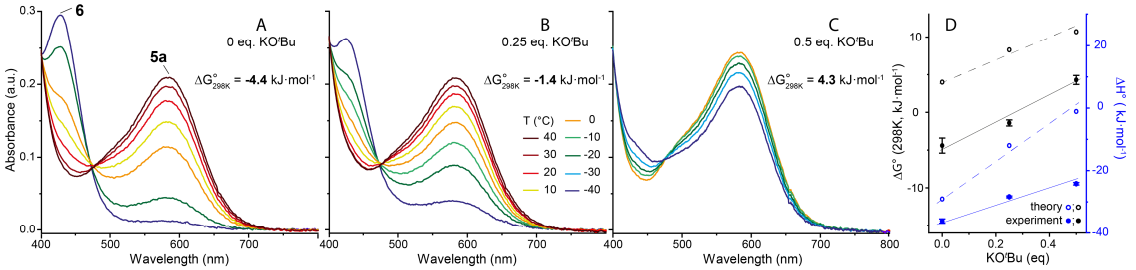

Figure 6. UV-vis spectra evolution and resulting thermodynamic parameters for the equilibrium of amido complex **5a** and hexanol in THF in the presence of KO^{t}Bu. A) Mn-**5a** (0.567mM) and hexanol (55.6 mM); B) Mn-**5a** (0.567mM), hexanol (113.4 mM), and KO^{t}Bu (28.35 mM, 0.25 eq. to hexanol); C) Mn-**5a** (0.567mM), hexanol (113.4 mM), and KO^{t}Bu (56.7 mM, 0.5 eq. to hexanol); D) Experimental (filled circles) standard reaction Gibbs free energy (black) and enthalpy (blue) changes associated with this equilibrium compared to theoretical (hollow circles) data (COSMO-RS, see Table S11).

The formation of metal (Ru, Fe, Os, Mn) alkoxide complexes have been frequently observed in hydride transfer reactions, especially in acceptorless dehydrogenative coupling, although their involvement in catalysis remains under debate.[19] Gusev and co-workers observed that the Ru alkoxide and hydride species can be present in equilibrium under the reaction conditions.[19c] On the other hand, Gauvin and co-workers considered an Mn alkoxide complex as an off-cycle intermediate that cause lower reactivity.[19g] The most detailed analysis to date was reported by the Saouma's group who investigated the relevance of the alkoxide complexes to the hydrogenation catalysis.[19h] The authors directly measured the equilibria of the formation of Ru-alkoxide and concluded the latter to compete with the H_2 addition to Ru amido complex. In the case of Mn-CNC, the alcohol binding can indeed explain the strong positive effect of elevated temperatures on catalysis. Apart from purely kinetic effect of rate acceleration, the increase in the reaction temperature suppresses the unfavorable alcohol binding and effectively changes the composition of the reaction mixture in favor of the kinetically competent catalyst state. While this implication is crucial for explaining temperature and substrate dependence of the ester hydrogenation at large, it leaves the role that base promoter in catalysis unexplained.

The requirement for the superstoichiometric amounts of base in ester and ketone hydrogenation is well documented. [8c, 19a, 19b, 19e, 20] Reports from the groups of Bergens, Morris and our group proposed that basic promoter could facilitate the H_2 activation.[19a, 19b, 20] We initially assume the role of the base (Table 1, entries1–3) to be purely kinetic with the base concentration affecting the initial rates of the hydrogenation. Our kinetic data, however, sharply contrasts that assumption. The

results presented in Figure 5C reveal nearly identical initial rates for the hexyl hexanoate hydrogenation in the presence of **2** and 10 mol% or 2 mol % KO^{t}Bu base suggesting no impact of the base concentration on the intrinsic catalytic kinetics. Instead, we observed a much more rapid decay of the hydrogenation rate, that was assigned to product inhibition, in the reduced base loading experiment suggesting that the same extent of inhibition could be reached at a lower conversion. The FTIR data confirmed that the identical inhibitory process was responsible for the rate decay. However, in a reduced base experiment a much higher concentration of the inhibited complex **6** was detected compared to the experiment with a high base loading (Figures 5F *vs*. 5D). This indicates that the presence of KO^{t}Bu can suppress the product inhibition, which is a highly unusual behavior that can only be consistent with thermodynamics if the two sets of reaction conditions are described by different equilibrium constants.

To verify whether the varied concentration of the base promotor can affect the thermodynamics of Mn alkoxide formation we tracked this transformation using temperature dependent UV-vis spectroscopy experiments were carried out. Strikingly, we found that the addition of substoichiometric amounts of KO^{t}Bu with respect to the alcohol reactant significantly impacts the standard Gibbs free energy change of the **5a** to **6** transformation (Figure 6). Note, that the base promotor is not involved directly in the equilibrium considered. Compared to the case of pure **5a**/alcohol system showing a negative ΔG°_{298K} of -4.4 kJ·mol^{-1} the addition of 0.25 equivalents of KO^{t}Bu with respect to the alcohol elevates the Gibbs free energy by approximately 3 kJ·mol^{-1} to -1.4 kJ·mol^{-1}, which increases further to 4.3 kJ·mol^{-1} upon the elevation of the base contents to 0.5 equivalents. These values remain valid even when we incorporate a likely exchange reaction between tert-butoxide and free hexanol in our calculation. Such a correction affects the obtained ΔG°_{298K} values by no more than 1 kJ·mol^{-1} suggesting a large magnitude of the alkoxide addition effect on the equilibria responsible for the catalyst inhibition.

These data strongly imply that even standard thermodynamic parameters often assumed constant are, in fact, condition dependent. Interestingly, this dependence can also be reflected in a theoretical analysis. We examined the energetics of the alkoxide formation using DFT calculations in combination with the COSMO-RS implicit solvation model. Initially, we validated this approach (see section S10 of the Supporting Information) by comparing the experiment and theory for the formation of Mn alkoxides in pure, base-free THF solvent (Table 2). We found that our analysis is sufficiently accurate for the larger HexOH and BnOH alcohols and less accurate for a short chain MeOH, that is a common limitation of the implicit solvation approach.[21] Extending this approach to the alkoxide formation in the presence of base we found that addition of alkoxide base can indeed affect the $\Delta G°$ of the reaction that formally does not involve this base as a reactant. The magnitude of this effect is

sufficient to perturb the reaction Gibbs free energy change by 4-8 kJ·mol^{-1} in line with our experimental observations depicted in Figure 6D. Interestingly this perturbation mainly stems from the change of the standard formation enthalpy and entropy of the alcohol component while metal complexes remain unaffected by the presence of the alkoxide base (see Table S11). Indeed, in aprotic solvent, one would expect the alcohol component to be affected stronger by the interaction with ionic alkoxide bases thus making this effect sensible from the molecular standpoint. Its magnitude and dramatic impact on catalysis is, however, novel and entirely unexpected.

Conclusion

In summary, this work describes two intrinsic phenomena that have profound influence on the outcome of the catalytic ester hydrogenation. First is the pronounced product inhibition developing throughout catalysis, caused by the reversible binding of the alcohol product to the catalyst. Demonstrating its capacity to severely diminish the steady state concentration of the catalytically competent species we expect this inhibitory pathway to be highly relevant for the early transition metal catalysts that tend to form more stable alkoxide complexes compared to their noble metal counterparts. In addition to showing the dynamic nature of catalyst species during the hydrogenation reaction, we demonstrate that even the standard thermodynamic parameters of the underlying elementary chemical transformations, often assumed ironclad, are strongly condition dependent. In our case, such a condition was the use of basic promotors. While we often rationalize the impact of the catalytic promoters in terms of stoichiometric reactivity, catalyst activation or acceleration of specific reaction steps, our work shows that the presence of promoter itself can dramatically affect the favorability of the catalytic reaction. Since promoters deliver this impact without the direct involvement in any chemical transformation, we stress the necessity to view them as an integral component of the reaction medium rather than a stoichiometric reagent. Finally, we conclude by noting that complexity uncovered in this work can potentially impact any related catalytic transformation involving reversible alcohol binding. Once reconciled, it can yield a powerful tool for designing catalytic reactions where favorability of elementary steps is no longer a perceived constant and can be tuned and manipulated at will.

References

1. (a) Rylander, P. N., *Catalytic Hydrogenation in Organic Syntheses: Paul Rylander*. Academic Press: New York, 1979; (b) Blaser, H. U.; Malan, C.; Pugin, B.; Spindler, F.; Steiner, H.; Studer, M., Selective hydrogenation for fine chemicals: Recent trends and new developments. *Adv. Synth. Catal.* **2003,** *345*, 103-151; (c) Vries, J. G. d., *The handbook of homogeneous hydrogenation*. Wiley-Vch: Weinheim, 2007; (d) McQuillin, F. J., *Homogeneous hydrogenation in organic chemistry*. Springer

311 Science & Business Media: 2012; Vol. 1; (e) Chaloner, P. A.; Esteruelas, M. A.; Joó, F.; Oro, L. A.,
312 *Homogeneous hydrogenation*. Springer Science & Business Media: 2013; Vol. 15; (f) Seo, C. S.; Morris,
313 R. H., Catalytic Homogeneous Asymmetric Hydrogenation: Successes and Opportunities.
314 *Organometallics* **2018,** *38*, 47-65.

315 2. (a) Clarke, M. L., Recent developments in the homogeneous hydrogenation of carboxylic acid
316 esters. *Catal. Sci. Technol.* **2012,** *2*, 2418-2423; (b) Werkmeister, S.; Junge, K.; Beller, M., Catalytic
317 hydrogenation of carboxylic acid esters, amides, and nitriles with homogeneous catalysts. *Org. Process*
318 *Res. Dev.* **2014,** *18*, 289-302; (c) Pritchard, J.; Filonenko, G. A.; van Putten, R.; Hensen, E. J.; Pidko, E. A.,
319 Heterogeneous and homogeneous catalysis for the hydrogenation of carboxylic acid derivatives:
320 history, advances and future directions. *Chem. Soc. Rev.* **2015,** *44*, 3808-3833; (d) Dub, P. A.; Batrice,
321 R. J.; Gordon, J. C.; Scott, B. L.; Minko, Y.; Schmidt, J. G.; Williams, R. F., Engineering catalysts for
322 selective ester hydrogenation. *Org. Process Res. Dev.* **2020,** *24*, 415-442.

323 3. (a) Kuriyama, W.; Matsumoto, T.; Ogata, O.; Ino, Y.; Aoki, K.; Tanaka, S.; Ishida, K.; Kobayashi,
324 T.; Sayo, N.; Saito, T., Catalytic hydrogenation of esters. Development of an efficient catalyst and
325 processes for synthesising (R)-1, 2-propanediol and 2-(l-menthoxy) ethanol. *Org. Process Res. Dev.*
326 **2012,** *16*, 166-171; (b) Spasyuk, D.; Smith, S.; Gusev, D. G., Replacing phosphorus with sulfur for the
327 efficient hydrogenation of esters. *Angew. Chem.* **2013,** *125*, 2598-2602; (c) Filonenko, G. A.; Cosimi, E.;
328 Lefort, L.; Conley, M. P.; Copéret, C.; Lutz, M.; Hensen, E. J.; Pidko, E. A., Lutidine-derived Ru-CNC
329 hydrogenation pincer catalysts with versatile coordination properties. *ACS Catal.* **2014,** *4*, 2667-2671;
330 (d) Filonenko, G. A.; Aguila, M. J. B.; Schulpen, E. N.; van Putten, R.; Wiecko, J.; Muller, C.; Lefort, L.;
331 Hensen, E. J. M.; Pidko, E. A., Bis-N-heterocyclic Carbene Aminopincer Ligands Enable High Activity in
332 Ru-Catalyzed Ester Hydrogenation. *J. Am. Chem. Soc.* **2015,** *137*, 7620-7623; (e) Tan, X.; Wang, Y.; Liu,
333 Y.; Wang, F.; Shi, L.; Lee, K.-H.; Lin, Z.; Lv, H.; Zhang, X., Highly efficient tetradentate ruthenium catalyst
334 for ester reduction: especially for hydrogenation of fatty acid esters. *Org. Lett.* **2015,** *17*, 454-457; (f)
335 Wang, Z.; Chen, X.; Liu, B.; Liu, Q.-b.; Solan, G. A.; Yang, X.; Sun, W.-H., Cooperative interplay between
336 a flexible PNN-Ru(II) complex and a $NaBH_4$ additive in the efficient catalytic hydrogenation of esters.
337 *Catal. Sci. Technol.* **2017,** *7*, 1297-1304; (g) He, T.; Buttner, J. C.; Reynolds, E. F.; Pham, J.; Malek, J. C.;
338 Keith, J. M.; Chianese, A. R., Dehydroalkylative activation of CNN-and PNN-pincer ruthenium catalysts
339 for ester hydrogenation. *J. Am. Chem. Soc.* **2019,** *141*, 17404-17413.

340 4. (a) Junge, K.; Wendt, B.; Jiao, H.; Beller, M., Iridium-Catalyzed Hydrogenation of Carboxylic Acid
341 Esters. *ChemCatChem* **2014,** *6*, 2810-2814; (b) Brewster, T. P.; Rezayee, N. M.; Culakova, Z.; Sanford,
342 M. S.; Goldberg, K. I., Base-free iridium-catalyzed hydrogenation of esters and lactones. *ACS Catal.*
343 **2016,** *6*, 3113-3117.

5. (a) Spasyuk, D.; Gusev, D. G., Acceptorless dehydrogenative coupling of ethanol and hydrogenation of esters and imines. *Organometallics* **2012,** *31*, 5239-5242; (b) Spasyuk, D.; Vicent, C.; Gusev, D. G., Chemoselective hydrogenation of carbonyl compounds and acceptorless dehydrogenative coupling of alcohols. *J. Am. Chem. Soc.* **2015,** *137*, 3743-3746.

6. (a) Zell, T.; Milstein, D., Hydrogenation and dehydrogenation iron pincer catalysts capable of metal–ligand cooperation by aromatization/dearomatization. *Acc. Chem. Res.* **2015,** *48*, 1979-1994; (b) Maji, B.; Barman, M. K., Recent Developments of Manganese Complexes for Catalytic Hydrogenation and Dehydrogenation Reactions. *Synthesis* **2017,** *49*, 3377-3393; (c) Alig, L.; Fritz, M.; Schneider, S., First-row transition metal (de) hydrogenation catalysis based on functional pincer ligands. *Chem. Rev.* **2018,** *119*, 2681-2751; (d) Filonenko, G. A.; van Putten, R.; Hensen, E. J.; Pidko, E. A., Catalytic (de) hydrogenation promoted by non-precious metals–Co, Fe and Mn: recent advances in an emerging field. *Chem. Soc. Rev.* **2018,** *47*, 1459-1483; (e) Gorgas, N.; Kirchner, K., Isoelectronic manganese and iron hydrogenation/dehydrogenation catalysts: Similarities and divergences. *Acc. Chem. Res.* **2018,** *51*, 1558-1569; (f) Irrgang, T.; Kempe, R., 3d-Metal Catalyzed N-and C-Alkylation Reactions via Borrowing Hydrogen or Hydrogen Autotransfer. *Chem. Rev.* **2018,** *119*, 2524-2549; (g) Kallmeier, F.; Kempe, R., Manganese Complexes for (De) Hydrogenation Catalysis: A Comparison to Cobalt and Iron Catalysts. *Angew. Chem. Int. Ed.* **2018,** *57*, 46-60; (h) Wang, Y.; Wang, M.; Li, Y.; Liu, Q., Homogeneous manganese-catalyzed hydrogenation and dehydrogenation reactions. *Chem* **2020,** *7*, 1180-1223.

7. (a) Elangovan, S.; Topf, C.; Fischer, S.; Jiao, H.; Spannenberg, A.; Baumann, W.; Ludwig, R.; Junge, K.; Beller, M., Selective catalytic hydrogenations of nitriles, ketones, and aldehydes by well-defined manganese pincer complexes. *J. Am. Chem. Soc.* **2016,** *138*, 8809-8814; (b) Kallmeier, F.; Irrgang, T.; Dietel, T.; Kempe, R., Highly active and selective manganese C= O bond hydrogenation catalysts: the importance of the multidentate ligand, the ancillary ligands, and the oxidation state. *Angew. Chem. Int. Ed.* **2016,** *55*, 11806-11809; (c) Garbe, M.; Junge, K.; Walker, S.; Wei, Z.; Jiao, H.; Spannenberg, A.; Bachmann, S.; Scalone, M.; Beller, M., Manganese(I)-Catalyzed Enantioselective Hydrogenation of Ketones Using a Defined Chiral PNP Pincer Ligand. *Angew. Chem. Int. Ed.* **2017,** *56*, 11237-11241; (d) Papa, V.; Cabrero-Antonino, J. R.; Alberico, E.; Spanneberg, A.; Junge, K.; Junge, H.; Beller, M., Efficient and selective hydrogenation of amides to alcohols and amines using a well-defined manganese–PNN pincer complex. *Chem. Sci.* **2017,** *8*, 3576-3585; (e) Garduño, J. A.; García, J. J., Non-Pincer Mn(I) Organometallics for the Selective Catalytic Hydrogenation of Nitriles to Primary Amines. *ACS Catal.* **2018,** *9*, 392-401; (f) Glatz, M.; Stöger, B.; Himmelbauer, D.; Veiros, L. F.; Kirchner, K., Chemoselective Hydrogenation of Aldehydes under Mild, Base-Free Conditions: Manganese Outperforms Rhenium. *ACS Catal.* **2018,** *8*, 4009-4016; (g) Kaithal, A.; Hölscher, M.; Leitner, W., Catalytic Hydrogenation of Cyclic Carbonates using Manganese Complexes. *Angew. Chem. Int. Ed.*

2018, *57*, 13449-13453; (h) Kumar, A.; Janes, T.; Espinosa-Jalapa, N. A.; Milstein, D., Manganese Catalyzed Hydrogenation of Organic Carbonates to Methanol and Alcohols. *Angew. Chem. Int. Ed.* **2018,** *57*, 12076-12080; (i) Weber, S.; Stöger, B.; Kirchner, K., Hydrogenation of nitriles and ketones catalyzed by an air-stable bisphosphine Mn (I) complex. *Org. Lett.* **2018,** *20*, 7212-7215; (j) Wei, D.; Bruneau-Voisine, A.; Chauvin, T.; Dorcet, V.; Roisnel, T.; Valyaev, D. A.; Lugan, N.; Sortais, J. B., Hydrogenation of Carbonyl Derivatives Catalysed by Manganese Complexes Bearing Bidentate Pyridinyl-Phosphine Ligands. *Adv. Synth. Catal.* **2018,** *360*, 676-681; (k) Zou, Y.-Q.; Chakraborty, S.; Nerush, A.; Oren, D.; Diskin-Posner, Y.; Ben-David, Y.; Milstein, D., Highly Selective, Efficient Deoxygenative Hydrogenation of Amides Catalyzed by a Manganese Pincer Complex via Metal–Ligand Cooperation. *ACS Catal.* **2018,** *8*, 8014-8019; (l) Buhaibeh, R.; Filippov, O. A.; Bruneau-Voisine, A.; Willot, J.; Duhayon, C.; Valyaev, D. A.; Lugan, N.; Canac, Y.; Sortais, J.-B., Phosphine-NHC Manganese Hydrogenation Catalyst Exhibiting a Non-Classical Metal-Ligand Cooperative H_2 Activation Mode. *Angew. Chem. Int. Ed.* **2019,** *58*, 6727-6731; (m) Freitag, F.; Irrgang, T.; Kempe, R., Mechanistic Studies of Hydride Transfer to Imines from a Highly Active and Chemoselective Manganate Catalyst. *J. Am. Chem. Soc.* **2019,** *141*, 11677-11685; (n) Wang, Y.; Zhu, L.; Shao, Z.; Li, G.; Lan, Y.; Liu, Q., Unmasking the ligand effect in manganese-catalyzed hydrogenation: mechanistic insight and catalytic application. *J. Am. Chem. Soc.* **2019,** *141*, 17337-17349; (o) Weber, S.; Stöger, B.; Veiros, L. F.; Kirchner, K., Rethinking Basic Concepts—Hydrogenation of Alkenes Catalyzed by Bench-Stable Alkyl Mn(I) Complexes. *ACS Catal.* **2019,** *9*, 9715-9720; (p) Weber, S.; Veiros, L. F.; Kirchner, K., Old Concepts, New Application–Additive-Free Hydrogenation of Nitriles Catalyzed by an Air Stable Alkyl Mn (I) Complex. *Adv. Synth. Catal.* **2019,** *361*, 5412-5420; (q) Zhang, L.; Tang, Y.; Han, Z.; Ding, K., Lutidine-Based Chiral Pincer Manganese Catalysts for Enantioselective Hydrogenation of Ketones. *Angew. Chem. Int. Ed.* **2019,** *58*, 4973-4977; (r) Garbe, M.; Budweg, S.; Papa, V.; Wei, Z.; Hornke, H.; Bachmann, S.; Scalone, M.; Spannenberg, A.; Jiao, H.; Junge, K., Chemoselective semihydrogenation of alkynes catalyzed by manganese(I)-PNP pincer complexes. *Catal. Sci. Technol.* **2020,** *10*, 3994-4001; (s) Papa, V.; Cao, Y.; Spannenberg, A.; Junge, K.; Beller, M., Development of a practical non-noble metal catalyst for hydrogenation of N-heteroarenes. *Nat. Catal.* **2020,** *3*, 135-142; (t) Zubar, V.; Sklyaruk, J.; Brzozowska, A.; Rueping, M., Chemoselective hydrogenation of alkynes to (Z)-alkenes using an air-stable base metal catalyst. *Org. Lett.* **2020,** *22*, 5423-5428; (u) Kaithal, A.; Werlé, C.; Leitner, W., Alcohol-Assisted Hydrogenation of Carbon Monoxide to Methanol Using Molecular Manganese Catalysts. *JACS Au* **2021,** *1*, 130-136; (v) Liu, C.; Wang, M.; Liu, S.; Wang, Y.; Peng, Y.; Lan, Y.; Liu, Q., Manganese-Catalyzed Asymmetric Hydrogenation of Quinolines Enabled by π–π Interaction**. *Angew. Chem. Int. Ed.* **2021,** *60*, 5108-5113; (w) Yang, W.; Chernyshov, I. Y.; van Schendel, R. K.; Weber, M.; Müller, C.; Filonenko, G. A.; Pidko, E. A., Robust and efficient hydrogenation of carbonyl compounds catalysed by mixed donor Mn (I) pincer complexes. *Nat. Commun.* **2021,** *12*, 1-8.

8. (a) Elangovan, S.; Garbe, M.; Jiao, H.; Spannenberg, A.; Junge, K.; Beller, M., Hydrogenation of Esters to Alcohols Catalyzed by Defined Manganese Pincer Complexes. *Angew. Chem. Int. Ed.* **2016,** *49*, 15364-15368; (b) Espinosa-Jalapa, N. A.; Nerush, A.; Shimon, L. J.; Leitus, G.; Avram, L.; Ben-David, Y.; Milstein, D., Manganese-Catalyzed Hydrogenation of Esters to Alcohols. *Chem. Eur. J.* **2017,** *23*, 5934-5938; (c) Van Putten, R.; Uslamin, E. A.; Garbe, M.; Liu, C.; Gonzalez-de-Castro, A.; Lutz, M.; Junge, K.; Hensen, E. J.; Beller, M.; Lefort, L., Non-Pincer-Type Manganese Complexes as Efficient Catalysts for the Hydrogenation of Esters. *Angew. Chem. Int. Ed.* **2017,** *56*, 7531-7534; (d) Widegren, M. B.; Harkness, G. J.; Slawin, A. M.; Cordes, D. B.; Clarke, M. L., A highly active manganese catalyst for enantioselective ketone and ester hydrogenation. *Angew. Chem. Int. Ed.* **2017,** *56*, 5825-5828; (e) Widegren, M. B.; Clarke, M. L., Towards practical earth abundant reduction catalysis: design of improved catalysts for manganese catalysed hydrogenation. *Catal. Sci. Technol.* **2019,** *9*, 6047-6058.

9. (a) Krieger, A. M.; Kuliaev, P.; Armstrong Hall, F. Q.; Sun, D.; Pidko, E. A., Composition-and Condition-Dependent Kinetics of Homogeneous Ester Hydrogenation by a Mn-Based Catalyst. *J. Phys. Chem. C.* **2020,** *124*, 26990-26998; (b) Kuliaev, P. O.; Pidko, E. A., Operando modeling of multicomponent reactive solutions in homogeneous catalysis: from non-standard free energies to reaction network control. *ChemCatChem* **2020,** *12*, 795.

10. Pfriem, N.; Hintermeier, P. H.; Eckstein, S.; Kim, S.; Liu, Q.; Shi, H.; Milakovic, L.; Liu, Y.; Haller, G. L.; Baráth, E., Role of the ionic environment in enhancing the activity of reacting molecules in zeolite pores. *Science* **2021,** *372*, 952-957.

11. (a) Kubis, C.; Selent, D.; Sawall, M.; Ludwig, R.; Neymeyr, K.; Baumann, W.; Franke, R.; Börner, A., Exploring Between the Extremes: Conversion-Dependent Kinetics of Phosphite-Modified Hydroformylation Catalysis. *Chem. Eur. J.* **2012,** *18*, 8780-8794; (b) Sherborne, G. J.; Chapman, M. R.; Blacker, A. J.; Bourne, R. A.; Chamberlain, T. W.; Crossley, B. D.; Lucas, S. J.; McGowan, P. C.; Newton, M. A.; Screen, T. E. O., Activation and deactivation of a robust immobilized Cp* Ir-transfer hydrogenation catalyst: a multielement in situ x-ray absorption spectroscopy study. *J. Am. Chem. Soc.* **2015,** *137*, 4151-4157; (c) Berry, D. B.; Codina, A.; Clegg, I.; Lyall, C. L.; Lowe, J. P.; Hintermair, U., Insight into catalyst speciation and hydrogen co-evolution during enantioselective formic acid-driven transfer hydrogenation with bifunctional ruthenium complexes from multi-technique operando reaction monitoring. *Faraday Discuss.* **2019,** *220*, 45-57; (d) Hall, A. M.; Dong, P.; Codina, A.; Lowe, J. P.; Hintermair, U., Kinetics of Asymmetric Transfer Hydrogenation, Catalyst Deactivation, and Inhibition with Noyori Complexes As Revealed by Real-Time High-Resolution FlowNMR Spectroscopy. *ACS Catal.* **2019,** *9*, 2079-2090; (e) Thomas, G. T.; Janusson, E.; Zijlstra, H. S.; McIndoe, J. S., Step-by-step real time monitoring of a catalytic amination reaction. *Chem. Commun.* **2019,** *55*, 11727-11730; (f) Bara-Estaún,

A.; Lyall, C. L.; Lowe, J. P.; Pringle, P. G.; Kamer, P. C.; Franke, R.; Hintermair, U., Multi-nuclear, high-pressure, operando FlowNMR spectroscopic study of Rh/PPh_3–catalysed hydroformylation of 1-hexene. *Faraday Discuss.* **2021,** *229*, 422-442.

12. Zhong, R.; Wei, Z.; Zhang, W.; Liu, S.; Liu, Q., A Practical and Stereoselective In Situ NHC-Cobalt Catalytic System for Hydrogenation of Ketones and Aldehydes. *Chem* **2019,** *5*, 1552-1566.

13. (a) Werkmeister, S.; Neumann, J.; Junge, K.; Beller, M., Pincer-Type Complexes for Catalytic (De) Hydrogenation and Transfer (De) Hydrogenation Reactions: Recent Progress. *Chem. Eur. J.* **2015,** *21*, 12226-12250; (b) Clarke, M. L.; Widegren, M. B., (2019). Hydrogenation reactions using Group III to Group VII transition metals. *Homogeneous Hydrogenation with Non-Precious Catalysts*, J. F. Teichert (Ed.).

14. Fu, S.; Shao, Z.; Wang, Y.; Liu, Q., Manganese-catalyzed upgrading of ethanol into 1-butanol. *J. Am. Chem. Soc.* **2017,** *139*, 11941-11948.

15. Ling, F.; Chen, J.; Nian, S.; Hou, H.; Yi, X.; Wu, F.; Xu, M.; Zhong, W., Manganese-catalyzed enantioselective hydrogenation of simple ketones using an imidazole-based chiral PNN tridentate ligand. *Synlett* **2020,** *31*, 285-289.

16. (a) Saudan, L. A.; Saudan, C. M.; Debieux, C.; Wyss, P., Dihydrogen reduction of carboxylic esters to alcohols under the catalysis of homogeneous ruthenium complexes: high efficiency and unprecedented chemoselectivity. *Angew. Chem. Int. Ed.* **2007,** *119*, 7473-7476; (b) Filonenko, G. A.; Cosimi, E.; Lefort, L.; Conley, M. P.; Coperet, C.; Lutz, M.; Hensen, E. J. M.; Pidko, E. A., Lutidine-Derived Ru-CNC Hydrogenation Pincer Catalysts with Versatile Coordination Properties. *ACS Catal.* **2014,** *4*, 2667-2671; (c) Fuentes García, J. A.; Smith, S.; Scharbert, M. T.; Carpenter, I.; Cordes, D. B.; Slawin, A. M. Z.; Clarke, M., On the functional group tolerance of ester hydrogenation and polyester depolymerisation catalysed by ruthenium complexes of tridentate aminophosphine ligands. *Chem. Eur. J.* **2015,** *21*, 10851-10860.

17. Morris, R. H., Ester hydrogenation catalyzed by a ruthenium(II) complex bearing an N-heterocyclic carbene tethered with an "NH_2" group and a DFT study of the proposed bifunctional mechanism. *ACS Catal.* **2013,** *3*, 32-40.

18. Tan, X.; Wang, Q.; Liu, Y.; Wang, F.; Lv, H.; Zhang, X., A new designed hydrazine group-containing ruthenium complex used for catalytic hydrogenation of esters. *Chem. Commun.* **2015,** *51*, 12193-12196.

19. (a) Abdur-Rashid, K.; Clapham, S. E.; Hadzovic, A.; Harvey, J. N.; Lough, A. J.; Morris, R. H., Mechanism of the hydrogenation of ketones catalyzed by trans-dihydrido (diamine) ruthenium (II) complexes. *J. Am. Chem. Soc.* **2002,** *124*, 15104-15118; (b) Hamilton, R. J.; Bergens, S. H., An unexpected possible role of base in asymmetric catalytic hydrogenations of ketones. Synthesis and characterization of several key catalytic intermediates. *J. Am. Chem. Soc.* **2006,** *128*, 13700-13701; (c) Bertoli, M.; Choualeb, A.; Lough, A. J.; Moore, B.; Spasyuk, D.; Gusev, D. G., Osmium and ruthenium catalysts for dehydrogenation of alcohols. *Organometallics* **2011,** *30*, 3479-3482; (d) Bielinski, E. A.; Förster, M.; Zhang, Y.; Bernskoetter, W. H.; Hazari, N.; Holthausen, M. C., Base-free methanol dehydrogenation using a pincer-supported iron compound and lewis acid co-catalyst. *ACS Catal.* **2015,** *5*, 2404-2415; (e) Alberico, E.; Lennox, A. J.; Vogt, L. K.; Jiao, H.; Baumann, W.; Drexler, H.-J.; Nielsen, M.; Spannenberg, A.; Checinski, M. P.; Junge, H., Unravelling the mechanism of basic aqueous methanol dehydrogenation catalyzed by Ru–PNP pincer complexes. *J. Am. Chem. Soc.* **2016,** *138*, 14890-14904; (f) Gusev, D. G., Dehydrogenative coupling of ethanol and ester hydrogenation catalyzed by pincer-type YNP complexes. *ACS Catal.* **2016,** *6*, 6967-6981; (g) Nguyen, D. H.; Trivelli, X.; Capet, F. d. r.; Paul, J.-F. o.; Dumeignil, F.; Gauvin, R. g. M., Manganese pincer complexes for the base-free, acceptorless dehydrogenative coupling of alcohols to esters: development, scope, and understanding. *ACS Catal.* **2017,** *7*, 2022-2032; (h) Mathis, C. L.; Geary, J.; Ardon, Y.; Reese, M. S.; Philliber, M. A.; VanderLinden, R. T.; Saouma, C. T., Thermodynamic Analysis of Metal–Ligand Cooperativity of PNP Ru Complexes: Implications for CO_2 Hydrogenation to Methanol and Catalyst Inhibition. *J. Am. Chem. Soc.* **2019,** *141*, 14317-14328.

20. Liu, C.; van Putten, R.; Kulyaev, P. O.; Filonenko, G. A.; Pidko, E. A., Computational insights into the catalytic role of the base promoters in ester hydrogenation with homogeneous non-pincer-based Mn-P, N catalyst. *Journal of Catalysis* **2018,** *363*, 136-143.

21. (a) Freire, M. G.; Ventura, S. P.; Santos, L. M.; Marrucho, I. M.; Coutinho, J. A., Evaluation of COSMO-RS for the prediction of LLE and VLE of water and ionic liquids binary systems. *Fluid Phase Equilib.* **2008,** *268*, 74-84; (b) Marenich, A. V.; Cramer, C. J.; Truhlar, D. G., Universal solvation model based on solute electron density and on a continuum model of the solvent defined by the bulk dielectric constant and atomic surface tensions. *J. Phys. Chem. B* **2009,** *113*, 6378-6396.

Acknowledgements

This research was supported by the European Research Council under the European Union's Horizon 2020 research and innovation program (grant agreement No. 725686). The use of the national computer facilities in this research was subsidized by NWO Domain Science. G.A.F. acknowledges NWO

for an individual Veni grant. All authors acknowledge BT Mass Spectrometry Facility at TU Delft for HRMS measurement

Author Contributions

All authors have given approval to the final version of the manuscript and declare no competing interests.